Engineering Stabilized Ion Channels: Covalent Dimers of Alamethicin[†]

Shaochun You,[‡] Shuyun Peng,[‡] Linda Lien,[‡] Jason Breed,[§] Mark S. P. Sansom,[§] and G. Andrew Woolley*

Department of Chemistry, University of Toronto, 80 St. George Street, Toronto, M5S 1A1, Canada, and Laboratory of Molecular Biophysics, University of Oxford, South Parks Road, Oxford, OX1 3QU, U.K.

Received December 12, 1995; Revised Manuscript Received March 11, 1996[⊗]

ABSTRACT: The peptide alamethicin forms channels with a variety of conductance states. Selective stabilization of a particular state should simplify the task of understanding conductance in terms of channel structure. We synthesized two different covalent dimers of alamethicin in which peptides were linked at their C-terminal ends by flexible tethers. Both dimeric peptides formed channels with conductances that matched those of alamethicin channels. Particular conductance states were selectively stabilized, however, with lifetimes up to 170-fold longer than the same states observed with monomers. In addition, tethering appeared to limit the size of the structures formed so that, even at higher peptide concentrations, a single predominant conductance state was obtained. We suggest this state corresponds to a channel made from six alamethicin molecules (three dimers).

The peptide alamethicin, from *Trichoderma viride*, has been studied intensively as a model ion channel (Latorre & Alvarez, 1981; Woolley & Wallace, 1992; Sansom, 1993b; Cafiso, 1994). Alamethicin can adopt a bent α-helical structure, and various lines of evidence indicate that a channel is formed by several such bent α-helices that self-assemble into a "barrel" or "bundle" structure that traverses the membrane. The recently reported structure of the acetylcholine receptor channel contains just such a bundle, composed of five bent α-helical segments (Unwin, 1995). The alamethicin channel can thus be viewed as a prototypic pore with all the surrounding mass of protein removed. A thorough understanding of the properties of such channels seems within the reach of current theory if an atomic description of the structure were available (Cooper et al., 1985; Eisenberg, 1995; Syganow & von Kitzing, 1995). To date, theories have been tested primarily with reference to the gramicidin channel system [*e.g.*, Roux and Karplus (1991)], the only well-defined system small enough to be computationally tractable. Unfortunately, gramicidin has a structure quite different from most ion channel proteins. In addition to providing a model for understanding ion permeation, an atomic description of the alamethicin channel could serve as a starting point for the design of channels with novel activities (Woolley et al., 1995).

The process of self-assembly of alamethicin channels does not lead to a unique number of peptide monomers per pore. Single-channel recordings of alamethicin show multiple conductance levels; frequent current steps are observed between adjacent levels. Boheim and others have suggested that the origin of these steps is the uptake and release of peptide monomers from a conducting bundle—the "barrel stave" model (Baumann & Mueller, 1974; Boheim, 1974)—that is, self-assembly is being directly observed through its effect on ion flux. Alternative explanations for the current steps include conformational changes or solvation changes in the conducting bundle (Hall, 1975; Fox & Richards, 1982; Hall et al., 1983) and/or the breakdown of correlated fluxes in a bundle of parallel pores (Gordon & Haydon, 1976; Berry & Edmonds, 1993).

Detailed understanding of the properties of this model ion channel would be facilitated if just one type of conducting structure could be selectively stabilized. If the "barrel stave" model is correct, then it should be possible to selectively stabilize a conducting state by defining the number of monomers in a barrel, *i.e.*, by chemically cross-linking monomers. Specification of oligomeric number by attachment of channel-forming peptides to templates [the "TASP" approach (Mutter, 1989)] has been reported for melittin (Pawlak et al., 1994), a synthetic proton-channel-forming peptide (Akerfeldt et al., 1993), and for several peptide segments of protein ion-channels (Akerfeldt et al., 1993; Oblatt-Montal et al., 1993). Given the wealth of structural and functional data on alamethicin and the quality of single-channel recording that can be obtained with this peptide, we felt that an analogous approach with alamethicin might lead to a particularly well-defined model ion channel. Preliminary reports of other attempts to link alamethicin helices have appeared (Leplawy et al., 1994; Marshall & Beusen, 1994, and references therein).

Since the stability of the alamethicin channel structure must presumably depend on a detailed close packing of adjacent helices (Sansom, 1993a), we were concerned that an inappropriate linker could impose restrictions on helix−helix packing and actually destabilize helix-bundles. At the outset, we felt the simplest approach would be to covalently link just two peptides with a flexible linker long enough to permit normal helix packing. The behavior of alamethicin derivatives with charged groups at the C-terminus has suggested that channels can form by N-terminal insertion and form all-parallel bundles of helices (Woolley et al., 1994). Cross-linking the C-terminal ends should not interfere, therefore, with channel formation. We have now synthesized C-terminal to C-terminal covalent dimers of

[†] This work has been supported by the Canadian Cystic Fibrosis Foundation, NSERC Canada, and the Wellcome Trust.

[‡] University of Toronto.

[§] University of Oxford.

[⊗] Abstract published in *Advance ACS Abstracts,* April 15, 1996.

S0006-2960(95)02921-7 CCC: $12.00

alamethicin (Rf50) with two different linkers (alm-PAPDA, alm-BAPHDA).[1] In both cases selective stabilization of specific current levels is observed. The current−voltage (I−V) relationships of these levels match those of channels formed by alamethicin monomers, indicating the linkers do not affect the pore structure of the channel. Tethering appears to limit the size of bundles formed so that only relatively small sized structures predominate. The most common state found at higher peptide concentrations has a lifetime 48-fold (alm-PAPDA) and 170-fold (alm-BAPHDA) longer than the corresponding state in channels formed from alamethicin monomers. We suggest this conducting state is a channel made from six alamethicin molecules (three dimers).

MATERIALS AND METHODS

Alamethicin was obtained from Sigma Chemical Co. Diphytanoyl-*sn*-glycero-3-phosphatidylcholine was purchased from Avanti Polar Lipids Inc. All other chemicals were obtained from Aldrich Chemical Co. and were the highest grade available.

Synthesis of the Linker, (Bis(N-3-aminopropyl)-1,7-heptanediamide (BAPHDA). A 25 mL dried flask was charged with 0.16 g (1 mmol) of pimelic acid, one drop of DMF, and 5 mL of CH_2Cl_2. The resulting suspension was cooled in an ice-water bath for 15 min. To it was added 0.31 mL (2.4 mmol) of oxalyl chloride, dropwise. The mixture was stirred at room temperature for 1 h to give a clear solution. The solvent and excess oxalyl chloride were evaporated, and the residue was redissolved in 5 mL of THF. Another dry 25 mL flask was charged with 3 mL of THF, 1.67 mL (20 mmol) of 1,3-diaminopropane, and 0.30 mL (2 mmol) of triethylamine. The mixture was cooled, and the solution of acid chloride prepared above was added dropwise. After addition, stirring was continued overnight. The mixture was then filtered and concentrated to give 0.102 g of crude product. This product was purified using an Alox column (2.5 × 10 cm) eluted first with 100 mL MeOH and then with 1 N NH_4OH in MeOH to give 81 mg of pure product. ^{1}H-NMR (D_2O, 200 MHz): 3.16 (t, 4H), 2.59 (t, 4H), 2.18 (t, 4H), 1.58 (m, 4H), 1.50 (m, 4H), 1.22 (m, 2H).

Synthesis of the Alamethicin−BAPHDA Dimer. A 10 mL dried flask was charged with 54 mg of *p*-nitrophenyl chloroformate, 1.8 μL of water, and 1 mL of THF. The mixture was cooled in an ice-water bath for 15 min. Triethylamine (0.1 mL) was then added dropwise to give an almost colorless suspension. A cooled solution of 8.1 mg of alamethicin [Rf50 (Gln^{18}), Sigma] in 2 mL of THF was added, and the mixture was stirred at 4 °C overnight. Water (0.1 mL) was then added to destroy unreacted *p*-nitrophenyl chloroformate and the corresponding anhydride. The resulting clear solution was stirred for 2 days at 4 °C. A solution of the linker (BAPHDA, 0.5 μmol) in DMF was then added. After being stirred at room temperature for an additional 2 days, this solution was passed through a gel filtration column

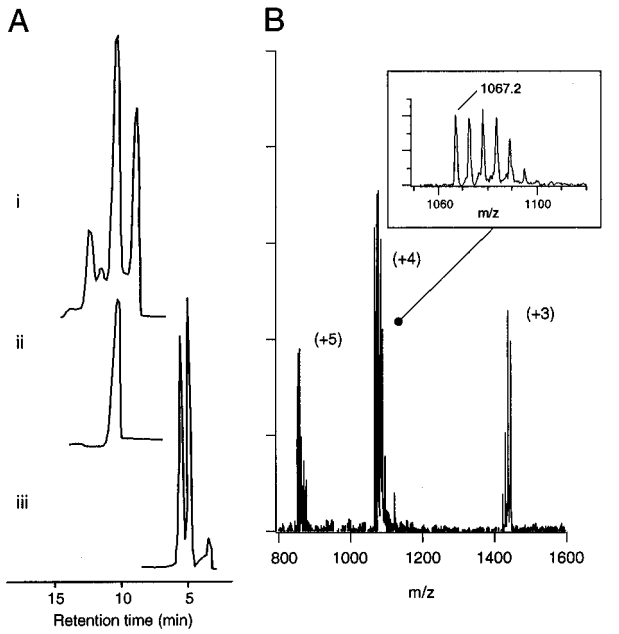

FIGURE 1: (A) HPLC chromatograms of (i) alm-BAPHDA, (ii) the central peak of i rechromatographed (this sample was used for mass spectrometry and ion channel measurements), and (iii) monomeric alamethicin Rf50 from Sigma. For chromatography conditions see text. (B) Electrospray mass spectrum of the HPLC purified alm-BAPHDA dimer (HPLC trace ii). Only one family of peaks (+5,+4,+3 charge states) is seen. Each charged species is also associated with a range of Na adducts (inset). The parent species has an observed average mass of 4264.8 daltons (calculated 4265.1).

(LH-20 in MeOH), and the first fraction, containing mainly dimer, was collected and concentrated. After lyophilization, 2.7 mg of crude dimer was obtained. This material was purified by reverse-phase HPLC (Zorbax C-18 column, 90% MeOH/10% H_2O, 0.1% TFA + TEA to pH 3). Unreacted monomer and monomer plus linker eluted well before the dimer fraction. The dimer appeared as a family of three peaks with areas in the approximate ratio 1:2:1 (Figure 1A). This was expected, since the monomeric peptide (Rf50 from Sigma) contains an approximately equal mixture of Ala^6- and Aib^6-alamethicin (Pandey et al., 1977), which are readily separated by reverse-phase HPLC (Figure 1A). The most prevalent dimer species contains one of each type of monomer. This was confirmed by electrospray mass spectrometry of the crude mixture which shows mass peaks in the same 1:2:1 ratio that differ by 14 mass units. This dimer species (the Aib^6−Ala^6 hybrid) was rechromatographed with the same solvent system for use in single-channel measurements. Electrospray MS of this peptide (Figure 1B) confirmed its purity and identity: observed molecular weight, 4264.8 (calculated, 4265.1)

Synthesis of Alamethicin Piperazine. A 10 mL dried flask was charged with 54 mg of *p*-nitrophenyl chloroformate, 1.8 μL of water, and 1 mL of tetrahydrofuran (THF). The mixture was cooled in an ice-water bath for 15 min. Triethylamine (0.1 mL) was then added dropwise to give an almost colorless suspension. A cooled solution of 8.1 mg of alamethicin [F50 (Gln^{18}), Sigma] in 2 mL of THF was added, and the mixture was stirred at 4 °C overnight. The suspension was filtered through Celite and added slowly to another 10 mL flask containing 100 equiv of piperazine, 100 μL of triethylamine, and 1 mL of THF cooled in an ice-water bath. The resulting suspension was stirred for 30 min and then concentrated to about 0.5 mL. This concentrated

[1] Abbreviations: Aib, aminoisobutyric acid; alm, alamethicin; alm-PA, alamethicin piperazine; BAPHDA, bis(*N*-3-aminopropyl)-1,7-heptanediamide; DCC, dicyclohexylcarbodiimide; DMF, dimethylformamide; FAB, fast atom bombardment; HOBt, hydroxybenzotriazole; HPLC, high-performance liquid chromatography; MS, mass spectrometry; MeOH, methanol; PAPDA, pimelic acid piperazine diamide; Pheol, phenylalaninol; THF, tetrahydrofuran; TEA, triethylamine.

solution was then passed through an LH-20 gel filtration column (3.4 × 18 cm) and eluted with methanol. The peptide-containing fractions were combined, concentrated, and lyophilized to give a white powder that was stored at −20 °C. Fast atom bombardment mass spectrometry (FAB-MS) gave the expected molecular weights: alm-PA, Ala^6 ($C_{97}H_{159}N_{25}O_{25}$), 2076; Aib^6, 2090.

Synthesis of Alamethicin−PAPDA Dimer. A 10 mL flask was charged with 4 mg (2 μmol) of alamethicin piperazine, 4.6 mg of HOBt, 12.4 mg of DCC and 1 mL of DMF. 160 μL (1 μmol) of pimelic acid solution in DMF (6.25 mM) was added, and the resulting mixture was stirred at room temperature for 4 days. The reaction mixture was passed through the LH-20 column and eluted with methanol. The first fraction, containing mainly dimer, was collected, concentrated, and lyophilized to give 1.2 mg of product. As with alm-BAPHDA, this material was purified by reverse-phase HPLC (Zorbax C-18 column, 92% MeOH/8% H_2O). The central peak of the dimer elution profile (retention time, 12 min) was collected, repurified under the same conditions, and characterized by electrospray MS: observed molecular weight, 4288.8 (calculated $C_{202}O_{52}N_{50}H_{328}$, 4289.13) (not shown).

Circular Dichroism. Spectra of the peptides in dioleoylphosphatidylcholine sonicated vesicles (1:20 mole ratio; concentrations determined by weighing the lyophilized powders) were recorded with an AVIV 62-DS spectropolarimeter using quartz cells of either 0.1 cm or 1 cm pathlength as described (Woolley et al., 1994). The spectropolarimeter was calibrated using (+)-10-camphorsulfonic acid, and all measurements were made at room temperature (22 ± 2 °C).

Single-Channel Measurements. Peptides (∼0.1 μM in MeOH) were added to both sides of membranes formed from diphytanoylphosphatidylcholine/decane (50 mg/mL) using established techniques (Seoh & Busath, 1993). Solutions were unbuffered 1 M KCl (pH = 5.8), and all measurements were made at 22 °C (±2 °C). Currents were measured and voltage was set using an Axopatch 1D patch-clamp amplifier (Axon Instruments). Data was filtered at either 2 kHz or 500 Hz, sampled at 5× the filter frequency, stored directly to disk, and analyzed using the program Synapse (Synergistic Research Systems). State lifetimes were estimated by maximum likelihood fitting of histograms of log(channel duration) using MacTac (Skalar Instruments) as described (Sigworth & Sine, 1987).

MOLECULAR MODELING

(1) Programs. Molecular dynamics (MD) simulations and model building were carried out using X-PLOR V3.1 (Brunger, 1992) with the CHARMM PARAM19 (Brooks et al., 1983) parameter set. Only H atoms attached to polar groups were represented explicitly; apolar groups were represented by extended atoms. Display and examination of models was carried out using Quanta V4.0 (Biosym-Molecular Simulations), and diagrams of structures were drawn using Molscript (Kraulis, 1991). Pore dimensions were calculated using HOLE (Smart et al., 1993). MD simulations were performed on DEC Alpha workstations, and all other calculations were carried out on Silicon Graphics workstations.

(2) Simulated Annealing via Restrained Molecular Dynamics. The method of simulated annealing via restrained molecular dynamics (SA/MD) has been described for modeling bundles of hydrophobic helices (Kerr et al., 1994). In stage 1 of SA/MD a Cα template was constructed corresponding to a bundle of six parallel helices, starting from the Cα coordinates of a single alamethicin helix [monomer C from the X-ray structure of Fox and Richards, (1982)]. The orientation of the helices within the helix-bundle is discussed below. Remaining backbone and side chain atoms were superimposed on the Cα atoms of the corresponding residues. These atoms "grew" from the Cα atoms, the positions of which remained fixed throughout stage 1. Annealing started at 1000 K, during which weights for bond lengths and bond angles, and subsequently for planarity and chirality, were slowly increased. A repulsive van der Waals term was introduced after an initial delay. Once the scale factors of these components of the empirical energy function reached their final values, the system was cooled from 1000 to 300 K, in steps of 10 K and 0.5 ps. During cooling, the van der Waals radii were reduced to 80% of their standard values in order to enable atoms to "pass by" one another. Electrostatic terms were *not* included during stage 1. Five structures are generated for each Cα template.

Structures from stage 1 were each subjected to 5 molecular dynamics runs (stage 2), resulting in an ensemble of 5 × 5 = 25 final structures. Initial velocities were assigned corresponding to 500 K. Harmonic positional restraints were imposed on Cα atoms at the beginning of stage 2 and were gradually relaxed as the temperature was reduced from 500 to 300 K. Distance restraints were also introduced at this point (see below). On reaching 300 K, a 5 ps burst of constant temperature dynamics was performed, followed by 1000 steps of conjugate gradient energy minimization. During the latter burst of dynamics and energy minimization no positional restraints were imposed on the Cα atoms. During stage 2 electrostatic interactions were introduced into the potential energy function. All main chain atoms are assigned partial charges as defined by the PARAM19 parameter set. Partial charges on side chain atoms of polar residues were gradually scaled up, from 0.05 to 0.4 times their full value, while the temperature was reduced from 500 to 300 K. A distance-dependent dielectric function was used, with a switching function in order to smoothly truncate distant (>9.5 Å) electrostatic interactions. Note that in each case the final scale factor (0.4) for polar side chain partial charges applied at the end of the 500 to 300 K cooling period was also used during the subsequent 5 ps burst of dynamics and energy minimization. The charge scaling procedure mimics electrostatic screening of charge−charge interactions within the transbilayer pore by water and counterions.

(3) Helix Orientations and Distance Restraints. In general, modeling a channel formed by a bundle of amphipathic helices requires several assumptions to be made (Kerr et al., 1994): (a) the number of helices in the bundle, *N*; (b) whether the helices run parallel or antiparallel to one another; (c) the orientation of the helices (by rotation about the helix long axis) relative to the center of the pore; and (d) in the case of kinked helices such as that of alamethicin, whether the N- or C-terminal helices are close packed within the bundle. In the SA/MD procedure these assumptions were embodied in the initial Cα-template and, to a lesser extent, in the distance restraints employed during stage 2. We now describe in detail the assumptions used in modeling channels formed by bundles of six helices, *i.e.*, by bundles of three

covalent dimers. These are based on consideration of a large body of experimental data for alamethicin [reviewed in, e.g., Woolley and Wallace (1992) and Sansom (1993b)].

The first assumption is that the channel is formed by six alamethicin monomers. This is not the only possible stoichiometry but is representative of the range of conductance levels observed for alamethicin and for alamethicin dimer channels (see Results). The assumption that neighboring helices in the bundle are approximately parallel, rather than antiparallel, is consistent with current models of alamethicin channel structure and gating and also with the maximum length of the covalent linker, which precludes antiparallel helix-bundles (see below). The orientation of the helices, as defined by rotation about their long axes, is based upon the reasonable assumption that the hydrophilic face of the alamethicin helix, as defined by residue Gln-7, is oriented toward the center of the pore. Note that this places the exposed carbonyl oxygen of Gly-11 and the C-terminal Gln-18 side chains in the pore lining. The final assumption concerns the packing of alamethicin helices within the bundle. The N-terminal segments of the helices are close-packed, while the C-terminal segments splay outward so as to form a wider channel mouth. By packing the helices in this manner it is possible for Gln-7 side chains to stabilize the helix-bundle by interhelix H-bonds. This was proposed by Fox and Richards (1982) on the basis of their crystal structure for alamethicin and has recently been confirmed experimentally by Molle et al. (1996) using various side chain substitutions at residue 7.

Intra- and interhelix distance restraints were imposed during stage 2. Both classes of restraint were implemented using the X-PLOR NOE potential energy function

$$E_{\mathrm{NOE}} = \min\left[E_{\mathrm{MAX}}, \frac{SK_{\mathrm{B}}T}{2\sigma^2}\right](d - d_{\mathrm{TARGET}})^2 \qquad (1)$$

with $E_{\mathrm{MAX}} = 20$ kcal/mol, $S = 2.5$, and $\sigma = 5.0$ Å for $d < d_{\mathrm{TARGET}}$ or $\sigma = 0.5$ Å for $d > d_{\mathrm{TARGET}}$. In this expression, d is the distance between the two restrained pseudoatoms and d_{TARGET} is the "target" distance for the restraint. Intrahelix restraints were used to maintain α-helical geometry and so acted between the carbonyl O of residue $i+4$ and the amide H of residue i. Target distances for these restraints were based α-helical H-bonding geometries observed in crystal structures of proteins (Baker & Hubbard, 1984).

Interhelix distances restraints acted between pairs of virtual atoms. These virtual atoms were defined as the geometric centers of two groups of Cα atoms, each group within one of a pair of helices. Two sets of interhelix restraints were applied to maintain the overall shape of the helix-bundle. The first was between the N-terminal segments of adjacent helices within a bundle (specifically between the geometric centers of atoms Cα:2−14 of helices i and $i+1$, with a target distance of $d_{\mathrm{TARGET}} = 10$ Å); the second was between helices on opposite sides of the bundle (between the geometric centers of atoms Cα:2−14 of helices i and $i+3$, with a target distance of $d_{\mathrm{TARGET}} = 20$ Å). The use of such restraints to bias helix packing toward a given overall geometry is discussed in more detail by Kerr et al. (1994). Studies on bundles of unmodified alamethicin helices (Breed et al., manuscript in preparation) suggest that the final structures yielded by SA/MD are not over-dependent on the value of d_{TARGET} employed.

(4) Modeling of Linkers. A hexameric bundle of linked alamethicin dimers was constructed by generating a Cα-template for an unmodified alamethicin bundle, using the criteria outlined above, to which a template for the three linkers was added. The linkers between adjacent helices of the three dimers making up the hexameric assembly were generated during the SA/MD procedure. X-PLOR topology patches were written to represent the covalent structure of the linkers. In the Cα-template the central methylene carbon of the linker was treated in a manner akin to that for the Cα atoms of the helices in that all the other atoms of the linker were initially superimposed upon it. However, its position was *not* fixed during SA/MD, thus allowing the conformation of the linker to be determined by its endpoints (i.e., links to the helices) and by the covalent structure of the linker as defined in the X-PLOR patch.

(5) Conductance Calculations. Maximum limiting conductances for the hexamer models were calculated by treating the pore as an irregular cylinder filled with electrolyte of constant resistivity. Integration of the resistance along the pore axis and addition of the access resistance at the mouths of the pore gives the total resistance, of which G_{max} is the inverse:

$$G_{\mathrm{max}} = \left[\frac{\rho}{4R_a} + \sum_a^b \frac{\rho}{\pi R^2}\,\mathrm{d}z + \frac{\rho}{4R_b}\right]^{-1} \qquad (2)$$

where the pore extends from $z = a$ to $z = b$, where R_a and R_b are the radii at the pore mouths, R the radius as a function of z in the pore, and where ρ is the resistivity of the electrolyte solution. Note that corrections for diffusion limitation, to be expected at higher voltages, and the effects of a potential barrier (*e.g.*, ion dehydration) are ignored in this simple model (Laver, 1994; Kuyucak & Chung, 1994; Sansom & Kerr, 1995). Thus the calculated conductance may be regarded as an upper limit.

RESULTS AND DISCUSSION

Design and Synthesis of Alamethicin Dimers. We wished to link two alamethicin monomers by their C-terminal ends in such a way that the link itself did not interfere with interhelical packing. Detailed modeling of various bundle geometries using the method of simulated annealing with molecular dynamics provided an estimate for the distance between the hydroxyl groups of the C-terminal phenylalaninol residues of the peptide in a channel (Breed & Sansom, 1994; Kerr et al., 1994; Breed et al., 1995). Two different linkers were then designed that could span this distance (PAPDA, pimelic acid piperazine diamide; BAPHDA, bis(*N*-3-aminopropyl)-1,7-heptanediamide (Figure 2). The BAPHDA linker is very flexible while the PAPDA linker is less so because of the two piperazine rings it contains. Synthesis of these dimers employed a novel carbamate-based coupling method that targeted the C-terminal hydroxyl group of alamethicin (see Materials and Methods section). Conversion of *p*-nitrophenyl chloroformate to the corresponding anhydride *in situ* permitted derivatization of this hydroxyl group without dehydrating Gln residues elsewhere in the peptide. Electrospray mass spectrometry was used to confirm the identity of the products after purification by HPLC. Circular dichroism spectra of the membrane-bound dimers had the same distinctive shape

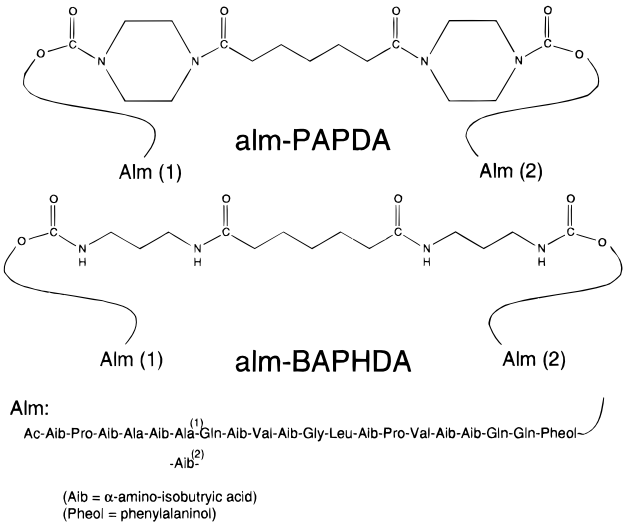

FIGURE 2: Primary structures of the alamethicin dimers.

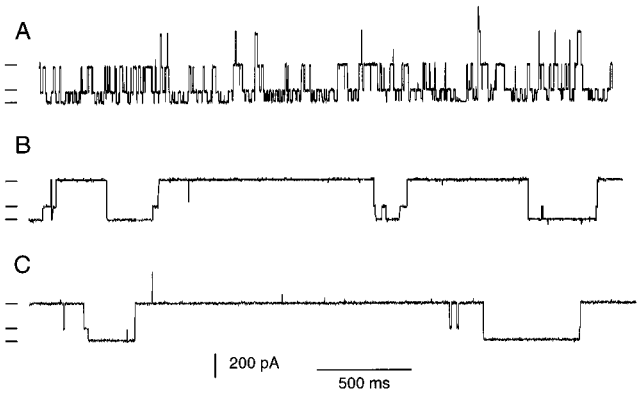

FIGURE 3: Continuous single-channel recordings of channels formed by alamethicin monomers (alm-Ala^{6}, Gln^{18}) (A), alm-PAPDA dimers (B), and alm-BAPHDA dimers (C). Conditions: 1 M KCl, pH 5.8, 160 mV, filtered at 2 kHz; diphytanoylphosphatidylcholine/decane membranes.

as that of alamethicin (Woolley & Wallace, 1992), indicating no major conformational effect of the linker (not shown). These dimers are designated alm-BAPHDA (alamethicin−bis(*N*-3-aminopropyl)-1,7-heptanediamide) and alm-PAPDA (alamethicin−pimelic acid piperazine diamide).

Single-Channel Measurements. Single-channel records of alm-BAPHDA, alm-PAPDA, and alamethicin itself in diphytanoyl-PC/decane membranes (1 M KCl, 160 mV, 22 °C) are shown in Figure 3. Under these conditions, each peptide forms channels with predominantly three different conductance states. With alm-PAPDA, channel events were occasionally observed with conductances larger by 10%−20% than those of the most common channels, but with the same overall appearance [*i.e.*, selective stabilization of particular levels (see below)]. Even with this variability, the current−voltage relations of the different conductance states of all three types of channel are nearly superimposable (Figure 4). This result is good evidence that the conformation of the conducting channel is minimally perturbed by the linker.

There are large differences, however, in the lifetimes of different states of dimer and monomer channels. This is immediately evident from the single-channel recordings in Figure 3. The upper and lower states of dimer channels appear to be selectively stabilized (levels 1 and 3); sojourns

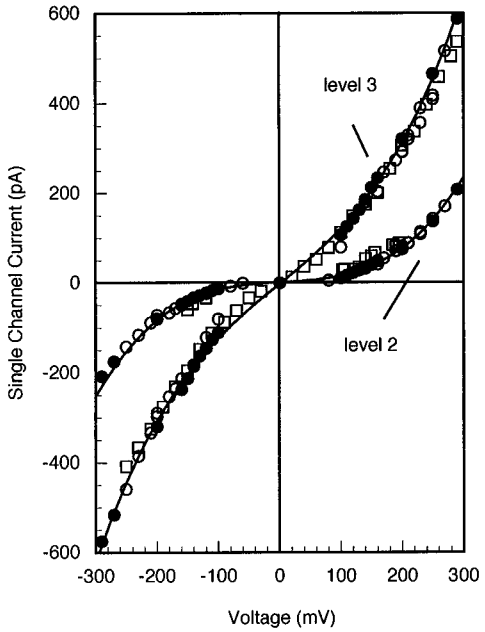

FIGURE 4: Single-channel current/voltage relations for channels formed by monomers (●), alm-PAPDA dimers (□), and alm-BAPHDA dimers (○) (1 M KCl, pH 5.8). Only the second and third conductance levels are shown; the first level is near zero on this scale. Peptides were added to both sides of the membrane.

in the intermediate state (level 2) are brief with a lifetime similar to the corresponding state of monomer channels.

Selective stabilization of alternate current levels can be rationalized by the barrel stave model as follows: Stabilization implies that the likelihood of a monomer either joining the conducting structure or leaving it is reduced. If a structure contains an integral number of dimers (an even number of monomers), then each monomer is tethered to part of the conducting structure. This should reduce the chance of a monomer leaving. In addition, a monomer that is part of an un-incorporated dimer must presumably join the conducting structure by inserting between two monomers in the helix-bundle. Insertion can only occur between two monomers that are not tethered, *i.e.*, there are half as many sites for insertion as there are in channels formed entirely of monomers. Conversely, stabilization should not occur if the conducting structure contains an odd number of monomers, that is, the tethered partner of one dimer is not actually part of the pore. Then, the current may readily step up a level if the un-incorporated, but tethered monomer joins the structure, or the current may step down a level if the monomer that is part of the pore, but not covalently connected to it, leaves.

If the concentration of alamethicin dimers is increased, or if the applied voltage is increased [see Wooley and Wallace (1992)], further step increases in single-channel current are seen. The distinctive feature of these is that they are all of the same size (shown for alm-BAPHDA in Figure 5A). In contrast, channels formed by alamethicin itself display current steps that continue to increase in size (Figure 5B). Apparently, tethering results in a preferred maximum size of the helix-bundle, so increasing the concentration of dimers increases the number of these bundles in the membrane instead of increasing the size of each bundle.

State 3, the preferred maximum conductance level, has a mean lifetime of 287 ms for alm-BAPHDA and 80 ms for alm-PAPDA, 170-fold and 48-fold longer, respectively, than

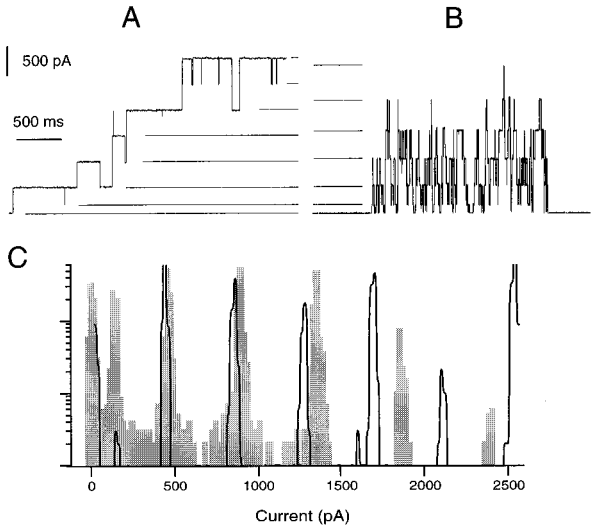

FIGURE 5: Single-channel currents of channels formed by alm-BAPHDA dimers (A) and monomers (B). Conditions as in Figure 3 except the voltage was 250 mV. Step changes in current are indicated by the horizontal bars. The same data in histogram format demonstrates that current steps of dimer-channels (outlines) are all of uniform size whereas those of monomer-channels increase in size (filled bars). The alm-PAPDA dimer shows similar behavior.

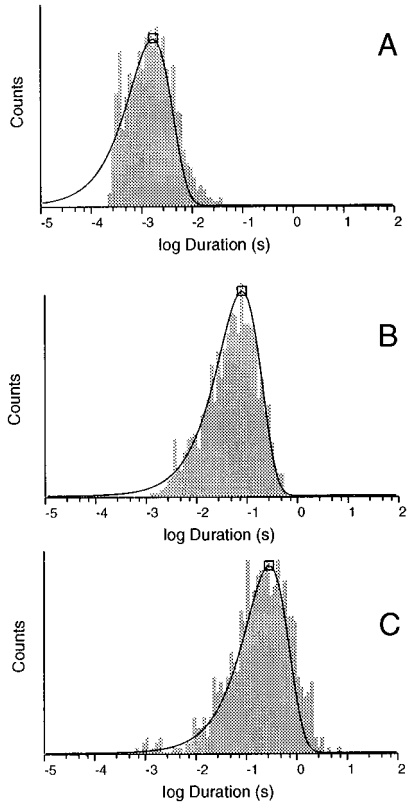

FIGURE 6: Duration histograms of state 3 of monomer-channels (A), alm-PAPDA dimers (B), and alm-BAPHDA dimers (C). Under the conditions of the experiments (160 mV, 1 M KCl), the majority of transitions from state 3 are to state 2; lifetimes appear to be well-described by a single time constant. Calculated mean lifetimes are 1.68 ms (monomer), 80 ms (alm-PAPDA), and 287 ms (alm-BAPHDA).

the corresponding state adopted by the unmodified alamethicin channel (Figure 6). Such changes in lifetime translate into relatively modest energy differences. It is not surprising, therefore, that the different linkers lead to somewhat different state lifetimes. These small changes are

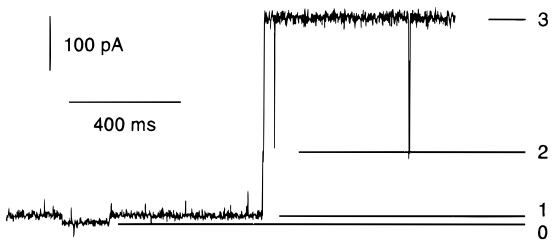

FIGURE 7: Expanded view of one channel formed by the alm-BAPHDA dimer showing a transition to the bare membrane conductance (state 0). The other conductance states are labelled. Conditions as in Figure 5.

sufficient nonetheless to greatly simplify the single-channel behavior.

Structural Interpretation. The fact that both dimers behave similarly and that the states they adopt correspond closely to states adopted by self-assembled monomers indicates that the role of the linkers is a benign stabilization of structures that occur, in any case, as a consequence of helix−helix packing. The single-channel records demonstrate the existence of homogeneous, well-defined channel structures formed by these tethered alamethicin molecules. State 3, in particular is consistently obtained when sufficient peptide is present. We now attempt to develop a structural model of this conducting state.

An examination of molecular models suggests that the smallest helix-bundle that contains a distinct pore is a 4-mer (Hanke & Boheim, 1980; Sansom, 1993b). The first current step observed in the present single-channel records is a transition from the bare membrane conductance to level 1 (Figure 7). We therefore tentatively assign level 1 to the 4-mer (two dimers). The intermediate level, which is less stable, is proposed to be an odd-numbered 5-mer, and the preferred upper state a 6-mer (three dimers).

Simulated annealing via restrained molecular dynamics was used to construct hexamer models as described previously for models built from monomeric peptides (Breed & Sansom, 1994; Kerr et al., 1994; Breed et al., 1995) (Figure 8). The results of these simulations suggest that the linker is flexible and does not significantly perturb the model of a hexameric bundle of alamethicin helices. Thus, although this model of the channel formed by the linked dimer is dependent upon the model of the channel formed by unlinked alamethicin monomers (Breed et al., manuscript in preparation), these simulations support the contention that the presence of the linker is compatible with the pre-existing pore geometry of an hexameric alamethicin helix-bundle. Examination of the individual helices reveals no significant differences in their structures between the linked and "unlinked" bundle models. In particular, examination of the corresponding Ramachandran plots provides no evidence for significant deviation from an overall α-helical structure in either model. Comparison of pore radius profiles shows that the presence of the linker increases the mean pore radius (averaged across an ensemble of 25 structures) by at most 0.25 Å relative to the unlinked bundle. This is less than the standard deviation for the variation in pore radius across either the linked or the unlinked ensemble, showing that the presence of the linker does not significantly perturb the dimensions of the pore structure in our simulations. Comparison of the geometries of helix packing between the linked and unlinked ensembles also fails to reveal any significant changes due to the linkers.

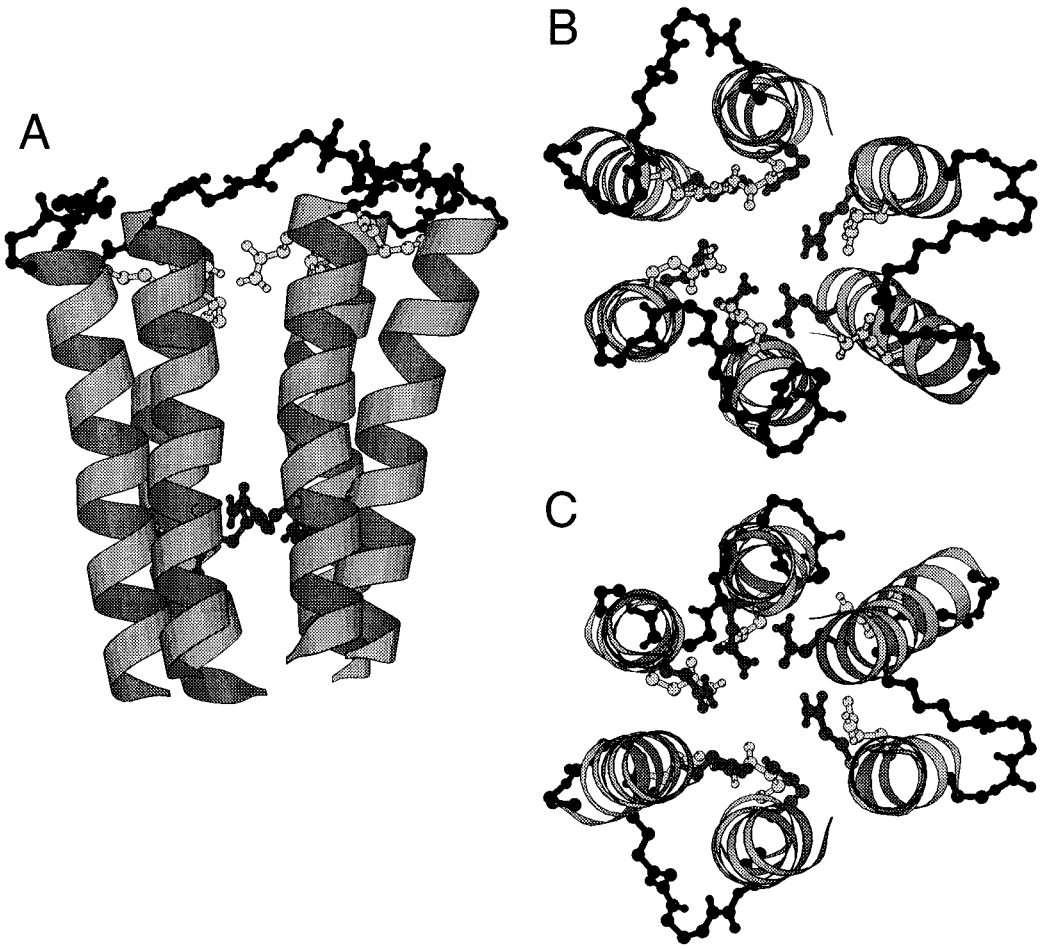

FIGURE 8: Model of the proposed hexamer channel (state 3) formed by three alm-BAPHDA dimers. Similar models can be built from alm-PAPDA dimers. The alamethicin backbone is represented as a ribbon, and the linkers are black. Glutamine side chains lining the pore are shown (Q18: light grey, Q7: dark grey). (A) Side view, (B) view down the pore from the C-terminal end, and (C) view from the N-terminal end. For a description of the modeling see text.

An all-parallel arrangement of helices is favored because the linker is too short to permit alternate helices to be antiparallel without significant distortions in helix packing. The possibility that one dimer is oriented differently than the other two cannot be completely excluded. Other, more complicated models are also possible [*e.g.*, multiple conductance pathways (Bezrukov & Vodyanoy, 1993)], but we feel they are not required at this stage to explain the available data.

An estimate of the conductance of such a structure can be made by treating the pore as an irregular cylinder of constant resistivity with corrections made for access resistance (see methods section). State 3 has an observed conductance of approximately 1 nS in 1 M KCl (measured at 100 mV; the I/V relations are somewhat supralinear). The conductance calculated from the models generated by simulated annealing, is very close to this value (0.9 ± 0.2 nS). For comparison, a conductance of approximately 140 pS would be expected for the hexamer in 150 mM NaCl. State 2, the putative 5-mer, would then have a conductance about one-third of this value (47 pS). The acetylcholine receptor channel, which is an established 5-mer, has a conductance of approximately 40 pS in 150 mM NaCl (Sachs, 1983), which is similar to the 5-mer level we propose. Although the exact nature of the pore lining will undoubtedly influence the conductance strongly, these simple calculations illustrate that the proposed structure could account for the observed conductance properties.

This putative hexameric pore has stability and conductance homogeneity comparable to that of the conformationally well-described gramicidin channel (Woolley & Wallace, 1992), although with significantly higher absolute conductance. The success of the cross-linking strategy indicates that pores containing different numbers of monomers could also be selectively stabilized. We are currently preparing covalent trimer and tetramer derivatives of alamethicin to test the models proposed here. The similarity of the architecture of these channels to those of protein ion-channels should make them relevant models for theoretical studies of biological ion permeation. The small size, conformational homogeneity, and chemical accessibility of these structures should permit both detailed simulation and detailed biophysical study (*e.g.*, by solid-state NMR) of their properties.

REFERENCES

Akerfeldt, K. S., Lear, J. D., Wasserman, Z. R., Chung, L. A., & DeGrado, W. F. (1993) *Acc. Chem. Res. 26*, 191−197.

Baker, E. N., & Hubbard, R. E. (1984) *Prog. Biophys. Mol. Biol. 44*, 97−179.

Baumann, G., & Mueller, P. (1974) *J. Supramol. Struct. 2*, 538−557.

Berry, R. M., & Edmonds, D. T. (1993) *J. Membr. Biol. 133*, 77−84.

Bezrukov, S. M., & Vodyanoy, I. (1993) *Biophys. J. 64*, 16−25.

Boheim, G. (1974) *J. Membr. Biol. 19*, 277−303.

Breed, J., & Sansom, M. S. P. (1994) *Biochem. Soc. Trans. 22*, 157S.

Breed, J., Kerr, I. D., Sankararamakrishnan, R., & Sansom, M. S. P. (1995) *Biopolymers 35*, 639−655.
Brooks, B. R., Bruccoleri, R. E., Olafson, B. D., States, D. J., Swaminathan, S., & Karplus, M. (1983) *J. Comp. Chem. 4*, 187−217.
Brunger, A. T. (1993) *X-PLOR, Version 3.1*, Yale University Press, New Haven CT.
Cafiso, D. S. (1994) *Annu. Rev. Biophys. Biomol. Struct. 23*, 141−165.
Cooper, K., Jakobsson, E., & Wolynes, P. (1985) *Prog. Biophys. Mol. Biol. 46*, 51−96.
Eisenberg, R. S. (1995) in *New Developments and Theoretical Studies of Proteins* (Elber, R., Ed.) World Scientific Publishing, Philadelphia, PA.
Fox, R. O., Jr., & Richards, F. M. (1982) *Nature 350*, 325−330.
Gordon, L. G. M., & Haydon, D. A. (1976) *Biochim. Biophys. Acta 436*, 541−556.
Hall, J. E. (1975) *Biophys. J. 15*, 934−939.
Hall, J. E., Vodyanoy, I., Balasubramanian, T. M., & Marshall, G. R. (1983) *Biophys. J. 45*, 233−248.
Hanke, W., & Boheim, G. (1980) *Biochim. Biophys. Acta 596*, 456−462.
Kerr, I. D., Sankararamakrishnan, R., Smart, O. S., & Sansom, M. S. P. (1994) *Biophys. J. 67*, 1501−1515.
Kraulis, P. J. (1991) *J. Appl. Crystallogr. 24*, 946−950.
Kuyucak, S., & Chung, S. (1994) *Biophysi. Chem. 52*, 15−24.
Latorre, R., & Alvarez, O. (1981) *Physiol. Rev. 61*, 77−150.
Laver, D. R. (1994) *Biophys. J. 66*, 355−359.
Leplawy, M. T., Kociolek, K., Slomczynska, U., Zabrocki, J., Beusen, D. D, & Marshall, G. R. (1994) *Pol. J. Chem. 68*, 969−974.
Marshall, G. R., & Beusen, D. D. (1994) in *Biomembrane Electrochemistry* (Blank, M., & Vodyanoy, I., Eds.) Advances in Chemistry Series 235, pp 259−314, American Chemical Society, Washington, DC.
Molle, G., Dugast, J. Y., Spach, G., & Duclohier, H. (1996) *Biophys. J. 70*, 1669−1675.
Mutter, M. (1989) *Angew. Chem., Int. Ed. Engl. 28*, 535−554.
Oblatt-Montal, M., Iwamoto, T., Tomich, J. M., & Montal, M. (1993) *FEBS Lett. 320*, 261−266.
Pandey, R. C., Cook, J. C., Jr., & Rinehart, K. L., Jr. (1977) *J. Am. Chem. Soc. 99*, 8469−8483.
Pawlak, M., Meseth, U., Dhanapal, B., Mutter, M., & Vogel, H. (1994) *Protein Sci. 3*, 1788−1805.
Roux, B., & Karplus, M. (1991) *Biophys. J. 59*, 961−981.
Sachs, F. (1983) in *Single-Channel Recording* (Sakmann, B., & Neher, E., Eds.) Plenum Press, New York.
Sansom, M. S. P. (1993a) *Eur. Biophys. J. 22*, 105−124.
Sansom, M. S. P. (1993b) *Q. Rev. Biophys. 26*, 365−421.
Sansom, M. S. P., & Kerr, I. D. (1995) *Biophys. J. 69*, 1334−1343.
Seoh, S., & Busath, D. (1993) *Biophys. J. 64*, 1017−1028.
Sigworth, F. J., & Sine, S. M. (1987) *Biophys. J. 52*, 1047−1054.
Smart, O. S., Goodfellow, J. M., & Wallace, B. A. (1993) *Biophys. J. 65*, 2455−2460.
Syganow, A., & von Kitzing, E. (1995) *J. Phys. Chem. 99*, 12030−12040.
Unwin, N. (1995) *Nature 373*, 37−43.
Woolley, G. A., & Wallace, B. A. (1992) *J. Membr. Biol. 129*, 109−136.
Woolley, G. A., Epand, R. M., Kerr, I. D., Sansom, M. S. P., & Wallace, B. A. (1994) *Biochemistry 33*, 6850−6858.
Woolley, G. A., Jaikaran, A. S. I., Zhang, Z., & Peng, S. (1995) *J. Am. Chem. Soc. 117*, 4448−4454.

BI9529216